Kinetic and Crystallographic Analysis of Mutant *Escherichia coli* Aminopeptidase P: Insights into Substrate Recognition and the Mechanism of Catalysis†

Stephen C. Graham,‡ Penelope E. Lilley,§ Mihwa Lee,‡ Patrick M. Schaeffer,§ Andrew V. Kralicek,§,|| Nicholas E. Dixon,§ and J. Mitchell Guss*,‡

School of Molecular and Microbial Biosciences, University of Sydney, NSW 2006, Australia, and Research School of Chemistry, Australian National University, ACT 0200, Australia

Received September 15, 2005; Revised Manuscript Received November 17, 2005

ABSTRACT: Aminopeptidase P (APPro) is a manganese-dependent enzyme that cleaves the N-terminal amino acid from polypeptides where the second residue is proline. APPro shares a similar fold, substrate specificity, and catalytic mechanism with methionine aminopeptidase and prolidase. To investigate the roles of conserved residues at the active site, seven mutant forms of APPro were characterized kinetically and structurally. Mutation of individual metal ligands selectively abolished binding of either or both Mn(II) atoms at the active site, and none of these metal−ligand mutants had detectable catalytic activity. Mutation of the conserved active site residues His243 and His361 revealed that both are required for catalysis. We propose that His243 stabilizes substrate binding through an interaction with the carbonyl oxygen of the requisite proline residue of a substrate and that His361 stabilizes substrate binding and the *gem*-diol catalytic intermediate. Sequence, structural, and kinetic analyses reveal that His350, conserved in APPro and prolidase but not in methionine aminopeptidase, forms part of a hydrophobic binding pocket that gives APPro its proline specificity. Further, peptides in which the required proline residue is replaced by *N*-methylalanine or alanine are cleaved by APPro, but they are extremely poor substrates due to a loss of interactions between the prolidyl ring of the substrate and the hydrophobic proline-binding pocket.

Aminopeptidase P (APPro;[1] EC 3.4.11.9) cleaves the N-terminal amino acid residue from polypeptide chains where the second residue is proline [P_1' residue, in the nomenclature of Schechter and Berger (*1*)]. This activity is of interest since many biologically active peptides, including coagulants, enzymes, growth factors, hormones, kinins, neurotransmitters, and toxins, have an N-terminal Xaa-Pro sequence (*2*). APPro is known to be directly involved in the regulation of one such biologically active peptide, the vasodilatory hormone bradykinin, and inhibitors of human APPro are promising cardiovascular therapeutic agents (*3*−*5*).

The crystal structure of *Escherichia coli* APPro has been solved to high resolution in four different space groups (*6*−*8*). *E. coli* APPro is a tetramer both in solution and in the crystalline form, each subunit containing a catalytic active site centered upon a dinuclear Mn(II) cluster (*6*). As predicted from sequence alignment (*9*), the C-terminal catalytic domain of APPro is structurally related to two other peptidases: the Xaa-Pro dipeptide-specific enzyme prolidase (*10*) and the Met-Xaa-... oligopeptide-specific enzyme methionine aminopeptidase (MetAP) (*11*). Based on their common fold, these enzymes are referred to as the "pita bread" metalloenzymes. Since they all share the same set of conserved active site residues and act upon similar substrates, it had been proposed that they share a conserved catalytic mechanism (*12*).

The nature and number of metal atoms required by pita bread metalloenzymes, and thus the precise roles of these metal atoms in catalysis, are topics of current debate. While the crystal structure of wild-type APPro reveals two Mn(II) atoms at the active site (*6*, *8*), human cytosolic APPro expressed in *E. coli* is active in the presence of only 1 molar equiv of Mn(II) (*13*), and porcine membrane-bound APPro is active in the presence of 1 molar equiv of Zn(II) (*14*). Spectroscopic and kinetic characterization of *E. coli* MetAP revealed that the metal site containing the imidazole ligand (equivalent to His354 in *E. coli* APPro) is "tight" and the other is "loose" (*15*). Under anaerobic conditions, catalysis occurs with a single Co(II) or Fe(II) atom in the tight site,

† This work was supported by the Australian Research Council (DP0208320 to J.M.G. and Hans C. Freeman). S.C.G. and M.L. are recipients of Australian Postgraduate Awards. Portions of this research were carried out at the Stanford Synchrotron Radiation Laboratory, a national user facility operated by Stanford University on behalf of the U.S. Department of Energy, Office of Basic Energy Sciences. The SSRL Structural Molecular Biology Program is supported by the Department of Energy, Office of Biological and Environmental Research, and by the National Institutes of Health, National Center for Research Resources, Biomedical Technology Program, and the National Institute of General Medical Sciences.

* To whom correspondence should be addressed: e-mail, m.guss@mmb.usyd.edu.au; tel, +61 2 9351 4302; fax, +61 2 9351 4726.

‡ University of Sydney.

§ Australian National University.

|| Present address: Molecular Olfaction Group, HortResearch, Mt. Albert Research Centre, Private Bag 92169, Auckland 1003, New Zealand.

[1] Abbreviations: APPro, aminopeptidase P; MetAP, methionine aminopeptidase; Lys(Abz)-Pro-Pro-pNA, L-lysyl(N^{ϵ}-2-aminobenzoyl)-L-prolyl-L-prolyl-4-nitroanilide; AHHpA-peptide, *N*-(2*S*,3*R*)-3-amino-2-hydroxyheptanoyl-L-alanyl-L-leucyl-L-valyl-L-phenylalanine methyl ester; AHMH-Pro, *N*-(2*S*,3*R*)-3-amino-2-hydroxy-5-methylhexanoyl-L-proline; apstatin, *N*-(2*S*,3*R*)-3-amino-2-hydroxy-4-phenylbutanoyl-L-prolyl-L-prolyl-L-alanine amide; MPD, 2-methyl-2,4-pentanediol; PEG 4K, poly(ethylene glycol) (average molecular weight 4000); rms, root mean square; SEM, standard error of the mean.

10.1021/bi0518904 CCC: $33.50
Published on Web 12/27/2005

and occupancy of the loose metal-binding site by Co(II) or Fe(II) reduces activity (*15*). Conversely, prolidase is virtually inactive in the presence of 1 equiv of Co(II) and requires a second Co(II) atom for full activity (*16*).

Attempts to study the metal requirement of pita bread metalloenzymes by mutation of metal ligands have produced equivocal results. A naturally occurring D219N mutant of yeast type I MetAP (equivalent to *E. coli* APPro D260N) maintains low levels of catalytic activity ($\sim 10^3$-fold less than wild type) and retains significant Co(II) binding affinity (0.43 versus 0.75 equiv for wild type) (*17*). Truncation of each metal ligand of *E. coli* MetAP to alanine yields mutants with residual activity (2−6% of wild type), yet none of these mutants retain stoichiometric levels of bound Co(II) (0.0−0.1 versus 1.6 equiv for wild type) (*18*). Mutation of any metal ligand of porcine membrane-bound APPro (Asp to Ala or Asn, Glu to Ala or Gln, His to Leu or Lys) gives completely inactive enzyme preparations (*19*). Further structural and kinetic investigations are required to clarify the effects of disturbing metal ligands upon the active site structure and catalytic activity of these enzymes.

Two nonmetal−ligand residues, His243 and His361, are conserved at the active sites of the pita bread metalloenzymes (Figure 3 of ref *20*) and are thought to play important roles in the catalytic mechanism. His361 has been implicated in stabilization of a *gem*-diol intermediate (*12*, *21*). His243 has been proposed to stabilize substrate binding via a hydrogen bond to the P_1' peptide nitrogen atom of the substrate (*21*), despite the fact that this hydrogen bond cannot be present when the P_1' residue is proline as required by APPro or prolidase (*8*, *20*). Mutation of the residues equivalent to His243 and His361 in porcine membrane-bound APPro to lysine or leucine yields inactive enzymes (*19*). Mutation of *E. coli* MetAP His79 (His243 in *E. coli* APPro) to alanine also abolishes activity (*22*). In the crystal structure of H79A MetAP, no metal ions were located at the active site, although metal binding was inferred from spectroscopic measurements (*22*). Mutation of *E. coli* MetAP His178 (His361 in *E. coli* APPro) to alanine does not affect the metal affinity of the enzyme (*23*), but H178A MetAP is 50−580-fold less active than the wild-type enzyme (*22*, *23*). Although extensive kinetic analysis of H178A MetAP suggested that His178 might be involved in water-mediated modulation of the Lewis acidity of the active site metal atoms (*23*), the mutant has not been characterized structurally.

The basis of proline specificity in APPro has also been the subject of close scrutiny. While APPro, prolidase, and MetAP all share the same fold, they have different substrate specificities. APPro and prolidase are specific for oligopeptides and dipeptides, respectively, with proline in the P_1' position. MetAP, on the other hand, prefers oligopeptides with methionine at the P_1 position and Gly, Ala, Ser, Thr, Pro, Val, or Cys at the P_1' position (*24*). Early studies on APPro and prolidase showed that proline specificity is not due to an ability to cleave cis peptide bonds (*25*, *26*). Structures of *E. coli* APPro in complex with substrate and product suggest that His350 and Arg404 form a hydrophobic pocket that recognizes the required substrate proline residue and that this rigid pocket cannot accommodate β-branched residues such as valine (*8*), but the inability of APPro to cleave peptides with smaller side chains (e.g., alanine) in the second position remains unexplained. The structure of dipeptidyl peptidase IV, which specifically removes dipeptides from oligopeptides where the second residue is proline, solved in complex with a peptide substrate showed that this enzyme has a well-conserved hydrophobic binding pocket that confers specificity for proline over alanine (*27*). Mutational and kinetic studies of the Pro-Xaa-specific enzyme prolyl aminopeptidase have shown that interaction between the prolidyl ring of a substrate and a hydrophobic proline-binding pocket at the active site of the enzyme is sufficient to confer a strong preference for Pro-Xaa substrates over Ala-Xaa or Gly-Xaa substrates (*28*). It is possible that the selectivity of APPro for Xaa-Pro peptides arises from a similar inability to bind substrates lacking a prolidyl ring at the P_1' position.

To address some of the outstanding issues of APPro catalytic mechanism and proline specificity, we have generated alanine mutants of seven conserved active site residues (His243, Asp260, Asp271, His350, His354, His361, and Glu383), measured their activities, and refined their crystal structures. We have also measured the affinity of wild-type APPro for substrates with alanine or *N*-methylalanine in the second position. Together, these kinetic and structural data confirm proposed catalytic roles for the conserved residues of APPro and define the basis of proline specificity in APPro and prolidase.

MATERIALS AND METHODS

Sequence Analysis. The full-length protein sequence of *E. coli* APPro was submitted to a BLAST (*29*) search of the UniProt knowledgebase [release 5.4, July 2005 (*30*)]. The 249 APPro and prolidase sequences most similar to *E. coli* APPro by BLAST search were aligned with CLUSTALX (*31*) using default parameters.

Generation, Expression, and Purification of APPro Mutants. Wild-type and mutant APPro were overexpressed in *E. coli* strain AN1459 containing plasmid pPL670 (*pepP*$^+$) and derivative plasmids, respectively, as described previously (*6*). Mutations in the *pepP* gene were generated using the QuikChange site-directed mutagenesis kit (Stratagene) and the mutagenic primers listed in Table S1 (see Supporting Information) and were confirmed by determination of the nucleotide sequences of the whole gene.

Wild-type APPro and mutant derivatives were purified as described previously (*8*), with minor modifications. Cells from 1.5 L of culture were resuspended in 30 mL of 50 mM Tris (pH 8.0) and 0.1 mM EDTA at 4 °C and lysed by treatment with lysozyme (Sigma) at 20 °C for 30 min followed by sonication. The lysate was cleared by centrifugation (48000*g*, 30 min, 4 °C). The cleared cell lysate was diluted to 100 mL in 20 mM Tris (pH 7.6), applied to an anion-exchange column (Toyopearl DEAE-650M; Tosoh), and eluted with a gradient of 0−1 M NaCl in 20 mM Tris (pH 7.6). Pooled eluate fractions were combined with an equal volume (12−30 mL) of 20 mM Tris (pH 7.6) and 3 M $(NH_4)_2SO_4$ before being applied to two EconoPac Methyl-HIC cartridges connected in series (Bio-Rad) and eluted with a gradient of 1.5−0 M $(NH_4)_2SO_4$ in 20 mM Tris (pH 7.6). Pooled HIC fractions were concentrated and exchanged into 20 mM Tris (pH 7.6) using Microsep centrifugal concentration devices (30 kDa MWCO; Pall). The final concentration of all APPro samples was $\sim$10 mg mL^{-1} as determined by

a Coomassie blue dye-binding assay (Bio-Rad). The purity of APPro samples (>98% for all samples) was confirmed by SDS−PAGE. Wild-type APPro used for kinetic studies with peptide substrates was subjected to size-exclusion chromatography in a Sephacryl S200 column (Pharmacia) that had been preequilibrated with 20 mM Tris (pH 7.6) and 150 mM NaCl. The recorded absorbance (λ = 280 mn) showed APPro as the only peak in the elution profile. Size-exclusion eluate was concentrated and exchanged into 20 mM Tris (pH 7.6) as described above.

Enzyme Kinetics. The activity of mutant APPro was assayed using the quenched fluorescent substrate Lys(Abz)-Pro-Pro-pNA (Bachem) (*32*). All enzyme preparations were freshly diluted with ice-cold 50 mM Tris (pH 8.1) and 100 mM NaCl and treated with $MnCl_2$ for 10 min at 37 °C prior to the assay. After addition of substrate, the final reaction conditions were 50 mM Tris (pH 8.1), 100 mM NaCl, 1 mM $MnCl_2$, 100 μM substrate, and 1 μg mL^{-1} APPro (final assay volume 250 μL). The assay was allowed to proceed for 30 min at 37 °C in a Wallac Victor^2 1420 fluorescent plate reader (Perkin-Elmer); the appearance of fluorescent product (λ_{ex} = 340 nm, λ_{em} = 430 nm) was monitored at 3 min intervals. Since the pure fluorescent product was not available to quantitate the changes in fluorescence, the kinetic results are presented as activities in relative fluorescence units (*8*). The values reported for k'_{cat} (maximal catalytic activity) are in units of fluorescence per minute per nanogram of APPro. The kinetic parameters K_M (Michaelis constant) and k'_{cat} (maximal catalytic activity) were determined using 5−200 μM Lys(Abz)-Pro-Pro-pNA and 1 μg mL^{-1} wild-type APPro or 4 μg mL^{-1} H350A APPro.

Competitive inhibition of Lys(Abz)-Pro-Pro-pNA hydrolysis by nonfluorogenic substrates was measured using a minor modification to the above protocol. Nonfluorogenic tripeptide substrates Ala-Pro-Ala, Ala-(*N*-methyl)Ala-Ala, and Ala-Ala-Ala were purchased from Bachem. The fluorogenic substrate Lys(Abz)-Pro-Pro-pNA and the nonfluorogenic peptide substrates were added to wild-type APPro that had been pretreated with $MnCl_2$ at 37 °C for 10 min. The final reaction conditions were 50 mM Tris (pH 8.1), 100 mM NaCl, 1 mM $MnCl_2$, 5 μM fluorogenic substrate, 0.1−5.0 mM nonfluorogenic tripeptide substrate, and 1 μg mL^{-1} APPro (final assay volume 250 μL). The reaction was monitored for 30 min at 37 °C as described above.

Activity of wild-type APPro with the nonfluorogenic peptide substrates Ala-Pro-Ala, Ala-(*N*-methyl)Ala-Ala, and Ala-Ala-Ala was measured using a slight modification of a previously published method (*33*). APPro was freshly diluted with ice-cold 50 mM Tris (pH 8.1) and 100 mM NaCl and treated with $MnCl_2$ for 15 min at 4 °C prior to the assay. After addition of substrate, the final reaction conditions were 50 mM Tris (pH 8.1), 100 mM NaCl, 1 mM $MnCl_2$, 0.31−3.75 mM tripeptide substrate, and 0.12 μg mL^{-1} wild-type APPro (final assay volume 80 μL). Due to the low activity of APPro against Ala-(*N*-methyl)Ala-Ala and Ala-Ala-Ala, higher final concentrations of APPro were required to quantify the activity (0.88 and 11.75 μg mL^{-1}, respectively). The reaction was allowed to proceed for 20 min at 37 °C, at which time 200 μL of ninhydrin reagent [1.6 g of ninhydrin in 80 mL of ethanol and 10 mL of glacial acetic acid, mixed with 1 g of $CdCl_2$ in 1 mL of water (*33*)] was added to each reaction. Samples were heated at 90 °C for exactly 15 min and then allowed to cool for 3 min before A_{492} was measured against a substrate blank. Concentrations of the product were quantified using a standard curve obtained with 0−0.3 mM alanine.

Kinetic parameters (K_M and k_{cat} or k'_{cat}) were obtained by fitting experimental data to the Michaelis−Menten equation by nonlinear regression using the program PRISM 4 (GraphPad Software). Apparent inhibitory constants (IC_{50}) were obtained by fitting experimental data to a sigmoidal dose−response curve by nonlinear regression using PRISM 4.

Protein Crystallization and X-ray Diffraction. Crystals were grown at 4 °C by vapor diffusion in hanging or sitting drops containing 2 μL of precipitant solution and 2 μL of APPro. Diffraction quality crystals grew within 1 month. Hexagonal crystals of mutant APPro (H243A, H354A, H361A) grew in hanging drops under conditions similar to those reported previously [6.1−6.6 mg mL^{-1} APPro, 0.1 M Tris (pH 8.2−8.5), 28−32% (w/v) PEG 4K (*6*)]. Hexagonal crystals were transferred to fresh drops containing reservoir solution supplemented with 1 mM $MnCl_2$ and cryoprotectant (10% v/v MPD) and allowed to equilibrate for 30−60 min prior to cryocooling. Tetragonal crystals of mutant APPro grew in sitting (D271A, H350A, E383A) or hanging (D260A) drops under conditions similar to those reported recently [7.1−18.3 mg mL^{-1} APPro, 0.1 M sodium citrate (pH 7.5), 0.2 M magnesium acetate, 28−30% (v/v) MPD (*8*)]. As these crystals were grown in MPD, they required no additional cryoprotection. They were transferred to fresh drops containing reservoir solution supplemented with 1 mM $MnCl_2$ and allowed to equilibrate for 30−60 min prior to cryocooling.

All crystals were flash cryocooled in a stream of N_2 gas (100 K) prior to data collection. Laboratory diffraction data were recorded at 100 K on a Mar345 imaging plate detector (Marresearch) using X-rays produced by a Rigaku RU200H rotating anode generator (Cu Kα, λ = 1.5418 Å), focused with Osmic mirrors (MSC Rigaku). Synchrotron diffraction data were recorded at the Stanford Synchrotron Radiation Laboratory beamline 9-2 (λ = 0.9809 Å) at 100 K on a Mar325 CCD detector (Marresearch). Diffraction data were indexed and integrated using MOSFLM (*34*) and scaled using SCALA (*35*).

Structure Solution and Refinement. The crystal structures were refined using the following protocol. Starting models were stripped of all nonprotein atoms (metals, solvent, hetero compounds). These models, treated as a rigid bodies, were refined using diffraction data to 3.0 Å resolution with REFMAC5 (*36*). The starting model for the refinement of H243A, H354A, and H361A APPro was the structure of Mn-loaded APPro refined in the hexagonal space group $P6_422$ [PDB ID 1WL9 (*8*)]. For D260A, D271A, H350A, and E383A APPro, the starting model was the structure of Na-loaded APPro refined in the tetragonal space group $I4_122$ [PDB ID 2BHC (*8*)].

Subsequent refinement involved iterative cycles of model building in COOT (*37*) using $F_o - F_c$ and $2F_o - F_c$ difference electron density maps followed by TLS (*38*) and restrained refinement in REFMAC5 (*36*) using all available diffraction data. Analysis and validation of all structures were carried out with the assistance of the program WHATCHECK (*39*) and the MOLPROBITY (*40*) server. Refinement restraints for modified cysteine residues and all hetero com-

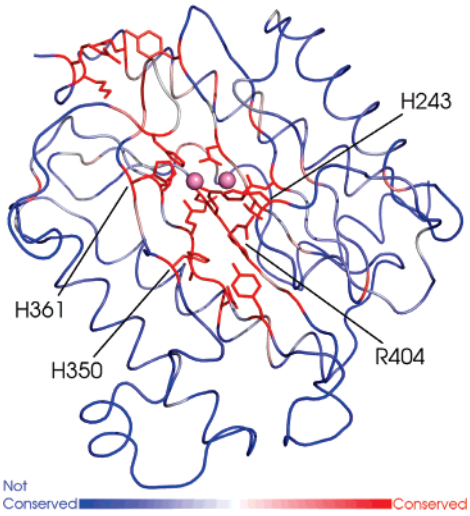

FIGURE 1: Sequence conservation of the pita bread domain of APPro and prolidase mapped onto the structure of the C-terminal domain of *E. coli* APPro. Each residue is colored by its conservation in 249 sequences of APPro and prolidase from blue (not conserved) to red (highly conserved). Side chains are shown only for strongly conserved residues. The Mn(II) atoms of the dinuclear metal site are shown in pink. PyMOL was used for molecular images (*47*).

pounds were generated with the assistance of the PRODRG (*41*) server. Superpositions and calculations of rms difference were performed using the program LSQMAN (*42*).

RESULTS

Residues at and around the Metal Center of APPro Are Highly Conserved. Inspection of the top 250 results returned from a BLAST search of the UniProt knowledgebase with *E. coli* APPro as the query sequence revealed 249 sequences that code for APPro or prolidase. A multiple alignment of these sequences, performed using the program CLUSTALX (*31*), is available as Supporting Information. Strong sequence conservation is evident for the C-terminal pita bread domain, whereas the N-terminal domain of *E. coli* APPro is not conserved. Mapping the sequence conservation onto the structure of the C-terminal domain of *E. coli* APPro (Figure 1) shows that the residues at and around the active site are the most conserved. As summarized in Table 1, all metal ligands are strictly conserved, as are His243 and His361, two residues previously identified as being important for catalysis (*6*, *22*). His350 and Arg404, which form extensive interactions with the prolidyl ring of bound substrate or product (*8*), are also strongly conserved (Table 1). Other conserved residues around the active site, not known to interact with the active site metals or substrate, are presumed to play structural roles in maintaining the integrity of the active site. On the basis of this sequence analysis, seven *E. coli* APPro mutants (with alanine substitutions at His243, Asp260, Asp271, His350, His354, His361, and Glu383) were generated to probe the substrate binding and catalytic mechanism of the enzyme.

H350A Is the Only APPro Mutant That Displays Significant Catalytic Activity. Of the seven mutant enzymes, only H350A displayed significant hydrolytic activity with Lys(Abz)-Pro-Pro-pNA as substrate (Figure 2). As wild-type and mutant APPro were overexpressed in *E. coli* without the aid of affinity tags, low levels of mutant APPro activity (less than 1% of wild-type activity) were not quantified because of possible contamination by endogenous wild-type enzyme. Catalytic activities of wild-type and H350A APPro were measured as a function of substrate concentration. H350A APPro exhibited lower substrate affinity (K_M = 140 ± 20 and 87 ± 8 μM for H350A and wild-type APPro, respectively) and lower maximal catalytic activity [k'_{cat} = 440 ± 40 and 5700 ± 200 fluorescence min^{-1} (ng of APPro)$^{-1}$ for H350A and wild-type APPro, respectively] than wild-type APPro. The observed k'_{cat}/K_M of H350A APPro was therefore 21-fold lower than for the wild-type enzyme.

Non-Proline Peptides Are Poor Substrates of APPro. The apparent inhibition of wild-type APPro Lys(Abz)-Pro-Pro-pNA hydrolysis by competition with the tripeptides Ala-Pro-Ala, Ala-(*N*-methyl)Ala-Ala, and Ala-Ala-Ala is shown in Figure 3. Ala-Pro-Ala reduces hydrolysis of Lys(Abz)-Pro-Pro-pNA with an apparent inhibitory constant (IC_{50}) of 0.22 ± 0.05 mM, while no inhibition is seen in the presence of Ala-(*N*-methyl)Ala-Ala or Ala-Ala-Ala.

The dependence of the activity of wild-type APPro on the concentrations of the tripeptide substrates Ala-Pro-Ala, Ala-(*N*-methyl)Ala-Ala, and Ala-Ala-Ala is presented in Figure 4. The kinetic parameters K_M (770 ± 50 μM), k_{cat} (85 ± 2 s^{-1}), and k_{cat}/K_M (110000 ± 9700 s^{-1} M^{-1}) of wild-type APPro with Ala-Pro-Ala as substrate are consistent with previously reported values (*43*). While wild-type APPro was able to hydrolyze the non-proline substrates Ala-(*N*-methyl)-Ala-Ala and Ala-Ala-Ala, individual kinetic parameters could not be obtained due to the limited sensitivity of the assay and the high apparent values of K_M (>4 mM, Figure 4). The activity of wild-type APPro depended linearly on substrate concentrations, giving approximate values of k_{cat}/K_M of 2260 ± 40 and 63 ± 4 s^{-1} M^{-1} for Ala-(*N*-methyl)Ala-Ala and Ala-Ala-Ala, respectively. Due to the lower activity of H350A APPro and limited sensitivity of the nonfluorogenic assay, measurement of H350A APPro activity with these tripeptide substrates was not attempted.

Molecular Structures of Mutant APPro. The structures of all seven site-directed mutants of *E. coli* APPro are reported at medium to high resolution (Table 2). Existence of the relevant mutation was confirmed in all structures during the early stages of refinement. Strong negative $F_o - F_c$ difference electron density was colocated with the side chain of the mutated residue in each model, and a lack of positive difference electron density confirmed that the side chain had not simply moved to another location. The overall structure of APPro is not significantly affected by the mutations. Excluding the C-terminal residues Lys439 and Gln440, which do not adopt a single conformation, the rms difference between the positions of 438 corresponding C$^{\alpha}$ atoms in wild-type [PDB ID 1WL9 (*8*)] and mutant APPro ranged from 0.09 to 0.30 Å. Structural differences between wild-type and mutant APPro were generally subtle and restricted to the close vicinity of the mutated residue.

Mutation of the metal−ligand residues at the active site resulted in selective elimination of binding of Mn_A, Mn_B, or both Mn(II) atoms (Figure 5). In E383A APPro, both Mn(II) atoms are present in the active site, but the bridging solvent molecule (W1) is located significantly farther from the metals than in wild-type APPro, and neither of the axial solvent atoms (W2 and W3) are present. In H354A APPro, Mn_B is present at the active site at less than full occupancy (0.75), and a water molecule (W_A) occupies the Mn_A site.

Table 1: Conservation of Active Site Residues of APPro, Prolidase, and MetAP

residue no. (*E. coli* APPro)	residue no. (*E. coli* MetAP)	notes
metal ligands		
Asp260	Asp97	strictly conserved
Asp271	Asp108	strictly conserved
His354	His171	strictly conserved
Glu383	Glu204	strictly conserved
Glu406	Glu235	this section of the catalytic domain is missing in a splice variant cDNA of prolidase from the marine sponge *Suberites domuncula* (UniProt ID O62566)
other residues		
His243	His79	strictly conserved
His350	N/A	not conserved in MetAP; conserved in all but five APPro/prolidase sequences, Ala in *Streptomyces lividans* APPro (UniProt ID P0A3Z4) and *Streptomyces coelicolor* APPro (UniProt ID P0A3Z3), Thr in two *Arabadopsis thaliana* hypothetical proteins (UniProt IDs Q9ZPZ5 and Q8GYQ0), and Cys in *Bifidobacterium longum* APPro (UniProt ID Q8G4M8); for all of these species except *B. longum* another APPro/prolidase gene sequence can be identified in which His350 is conserved
His361	His178	Arg in the prolidase from *Bdellovibrio bacteriovorus* (UniProt ID Q6MN88)
Arg404	N/A	not conserved in MetAP; this section of the catalytic domain is missing in a splice variant cDNA of prolidase from the marine sponge *S. domuncula* (UniProt ID O62566)

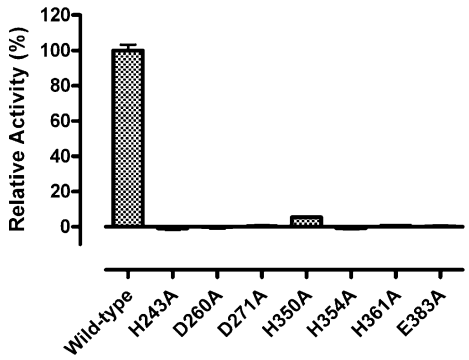

FIGURE 2: Relative activity of wild-type and mutant APPro. Activity was measured using the quenched fluorescent substrate Lys(Abz)-Pro-Pro-pNA. Each bar represents the mean of five independent measurements (±SEM).

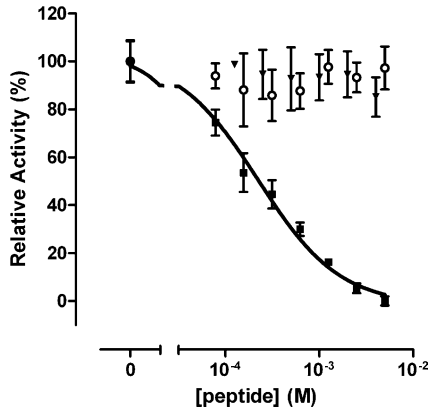

FIGURE 3: Plot of relative activity of wild-type APPro with Lys-(Abz)-Pro-Pro-pNA vs concentration of the tripeptide competitive substrates Ala-Ala-Ala (▼), Ala-(*N*-methyl)Ala-Ala (○), and Ala-Pro-Ala (■). Each point represents the mean of three independent measurements (±SEM). The curve represents a nonlinear regression fit of the entire data set for the apparent inhibition by Ala-Pro-Ala to a sigmoidal dose−response curve.

The bridging solvent (W1) is 2.1 Å from Mn_B and 2.7 Å from W_A. The axial solvent molecule (W3) is farther from Mn_B (2.8 Å) than the equivalent molecule in wild-type APPro (2.4 Å). In D260A APPro, Mn_A is bound at the active site, but the Mn_B site is empty. In this case, the limited resolution of the structure determination (d_{min} = 2.9 Å) did not permit the modeling of any solvent bound to Mn_A. Lastly, in D271A APPro no atoms of Mn(II) are bound at the active site. One Na(I) atom, coordinated by His354, Glu383, Glu406, and two solvent atoms, was modeled at the active site based on the height of difference electron density and geometric considerations. The side chain of Glu383 is rotated significantly around the $C^{\gamma}-C^{\delta}$ bond in order to accommodate the bound Na(I) atom. The active site of D271A APPro is highly disordered, and the possibility of heterogeneity at the metal site cannot be discounted.

The binding of metal atoms is not significantly affected by mutation of nonmetal−ligand residues, although these mutations do cause rearrangement of bound solvent molecules at the active site (Figure 6). The metal site of H350A APPro is indistinguishable from that of the wild-type enzyme within experimental error. The only difference between the metal sites of H243A and wild-type APPro is that the solvent molecule W2 is located farther from Mn_A than in wild-type APPro, although it maintains the same hydrogen bonds to W1 and $N^{\epsilon 2}$(His361). In H361A APPro, W2 is not seen.

In some of the structures, minor rearrangement of nearby residues occurs as a result of the mutation. In D260A APPro, the side chain of Arg404, which forms a hydrogen bond with $O^{\delta 2}$(Asp260) in wild-type APPro, is rotated around the $C^{\alpha}-C^{\beta}$ bond and N^{ϵ}(Arg404) now forms a hydrogen bond to O^{γ}-(Thr273). (O^{γ}(Thr273) also forms a hydrogen bond with the carboxylate group of Asp260 in wild-type APPro.) In H354A APPro, the peptide bond between the residues Val360 and His361 is flipped. Val360 adopts a different rotamer conformation, and the imidazole side chain of His361 is located 1 Å closer to the metal site than the equivalent side chain in wild-type APPro. His361 could not occupy this position in the wild-type enzyme because it would clash with the side chain of His354. In H361A APPro, the carboxylate side chain of Asp38 from an adjacent monomer, which forms a hydrogen bond with $N^{\delta 1}$(His361) of wild-type APPro, is rotated 120° around the $C^{\alpha}-C^{\beta}$ bond and no longer faces the active site (Figure 6).

Some of the APPro mutants crystallized with buffer components bound at the active site. In E383A APPro a sulfate ion is bound (occupancy = 0.70), forming a strong hydrogen bond (2.5 Å) with $N^{\epsilon 2}$(His243). The structures of D260A and H350A APPro both have one molecule of MPD bound at the active site. In D260A APPro the MPD occupies

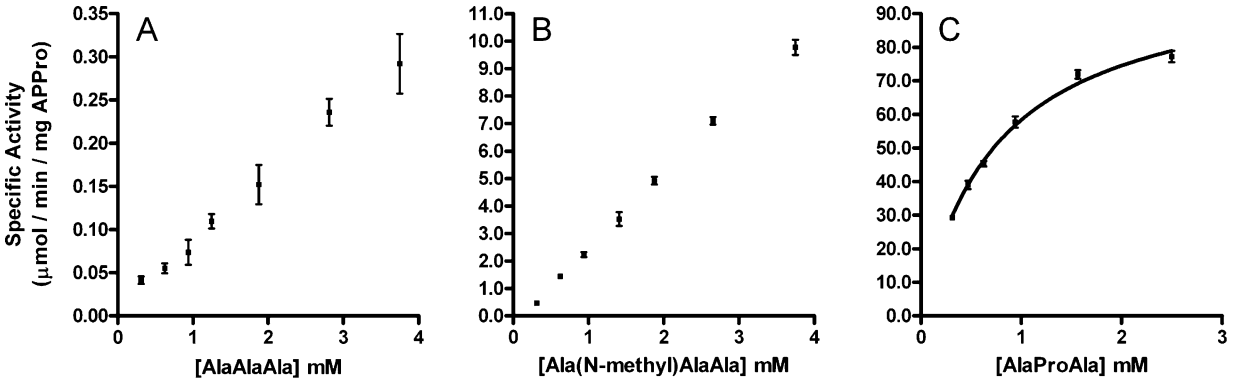

FIGURE 4: Plot of wild-type APPro specific activity (micromoles of product formed per minute per milligram of enzyme) vs concentration of the tripeptide substrates: (A) Ala-Ala-Ala, (B) Ala-(*N*-methyl)Ala-Ala, and (C) Ala-Pro-Ala. Each point represents the mean of five independent measurements (±SEM). The curve represents a nonlinear regression fit of the entire data set to the Michaelis−Menten equation.

Table 2: Data Collection and Refinement Statistics

crystal	H243A APPro	D260A APPro	D271A APPro	H350A APPro	H354A APPro	H361A APPro	E383A APPro
			Crystal and Diffraction Data				
pH	8.2	7.5	7.5	7.5	8.5	8.5	7.5
space group	$P6_422$	$I4_122$	$I4_122$	$I4_122$	$P6_422$	$P6_422$	$I4_122$
unit cell dimensions							
a (Å)	177.2	137.6	138.6	138.2	177.3	177.3	138.6
c (Å)	96.4	232.0	232.1	231.3	96.8	96.5	231.4
X-ray source	rotating anode	SSRL BL9-2	SSRL BL9-2	rotating anode	rotating anode	rotating anode	rotating anode
λ (Å)	1.5418	0.9809	0.9809	1.5418	1.5418	1.5418	1.5418
resolution range (Å)	76.7−1.75 (1.84−1.75)[a]	24.1−2.9 (3.06−2.90)	22.6−2.2 (2.32−2.20)	74.5−2.6 (2.74−2.60)	76.7−1.7 (1.79−1.70)	65.2−1.7 (1.79−1.70)	60.0−2.4 (2.53−2.40)
unique reflections	86631 (12594)	22735 (3362)	56922 (8253)	33663 (4324)	97989 (14128)	96986 (13977)	41368 (5806)
completeness (%)	97.3 (97.9)	91.7 (94.5)	99.4 (100.0)	97.2 (86.6)	100.0 (100.0)	99.4 (99.5)	94.1 (91.3)
multiplicity	5.0 (3.5)	3.8 (3.7)	4.1 (4.1)	5.4 (4.6)	5.9 (5.1)	6.0 (5.1)	5.9 (4.5)
$\langle I/\sigma(I)\rangle$	17.4 (3.4)	10.50 (2.0)	13.60 (1.8)	14.0 (2.4)	16.5 (1.9)	19.7 (2.8)	13.9 (2.5)
R_{merge}[b]	0.06 (0.29)	0.10 (0.53)	0.06 (0.55)	0.11 (0.59)	0.07 (0.67)	0.06 (0.48)	0.11 (0.55)
			Refinement Statistics				
reflections in working set	83997	21640	53699	32029	94990	94042	39342
reflections in test set	2632	1091	2799	1630	2965	2938	2026
total atoms (non-H)	4181	3569	3689	3681	4185	4199	3712
protein atoms	3495	3484	3484	3484	3495	3495	3483
metal atoms	2	2	2	3	1	2	3
water atoms	642	41	169	152	636	647	187
atoms in alternate conformers	41	21	13	21	52	54	21
other atoms[c]	1	21	21	21	1	1	18
R_{cryst}[d]	0.150 (0.242)	0.169 (0.322)	0.170 (0.303)	0.172 (0.295)	0.158 (0.294)	0.150 (0.302)	0.172 (0.325)
R_{free}[e]	0.165 (0.299)	0.202 (0.387)	0.193 (0.303)	0.204 (0.364)	0.176 (0.359)	0.165 (0.364)	0.207 (0.370)
rmd, bond lengths (Å)	0.009	0.008	0.010	0.010	0.010	0.010	0.010
rmd, bond angles (deg)	1.160	1.074	1.181	1.181	1.183	1.206	1.178
$\langle B\rangle$ (Å^2)	21.8	66.3	57.5	44.3	18.6	21.0	38.4
DPI (Å)[f]	0.07	0.36	0.12	0.21	0.06	0.06	0.17
PDB ID	2BWS	2BWT	2BWU	2BWW	2BWX	2BWV	2BWY

[a] The values in parentheses are for the highest resolution shell. [b] $R_{merge} = \sum_h\sum_i|I_{hi} - \langle I_h\rangle|/\sum_h\sum_i\langle I_h\rangle$. [c] Includes atoms of buffer or anions. [d] $R_{cryst} = \sum_h|F_h(\text{obs}) - F_h(\text{calc})|/\sum_h F_h(\text{obs})$. [e] $R_{free} = R_{cryst}$ for approximately 5% of the data not used during refinement. The sets of test reflections were the same as those used for the refinements of the published starting models: PDB ID 1WL9 (*8*) for structures in the hexagonal space group $P6_422$ and PDB ID 2BHC (*8*) for structures in the tetragonal space group $I4_122$. [f] DPI is the diffraction precision indicator defined by Cruickshank (*46*).

the same general position as in Zn-loaded APPro (*8*) but forms different hydrogen bond interactions. In H350A APPro the MPD molecule occupies the position of the imidazole side chain of His243 in wild-type APPro (Figure 6). As a result, the side chain of His243 is rotated around its $C^{\alpha}-C^{\beta}$ bond and is located farther from the metal site than in wild-type APPro. The *B* values of the imidazole side chain of His243 refine to high values, indicating that the side chain is disordered. It was observed previously that the position of His243 responds to the presence of different ligands bound at the active site (*8*). The disorder in the active site of H350A APPro extends to residues 87−91 in an adjacent subunit. The peptide bond between residues Trp88 and Phe89, the O(peptide) atom of which forms a hydrogen bond with the N(peptide) of His243 in wild-type APPro, was not located in electron density and was not modeled.

DISCUSSION

As originally identified by sequence analysis (*9*), APPro shares a common pita bread fold with the other exopeptidases prolidase and MetAP (*6*, *10*, *11*). The active site structures of the three enzymes are almost identical, with two divalent

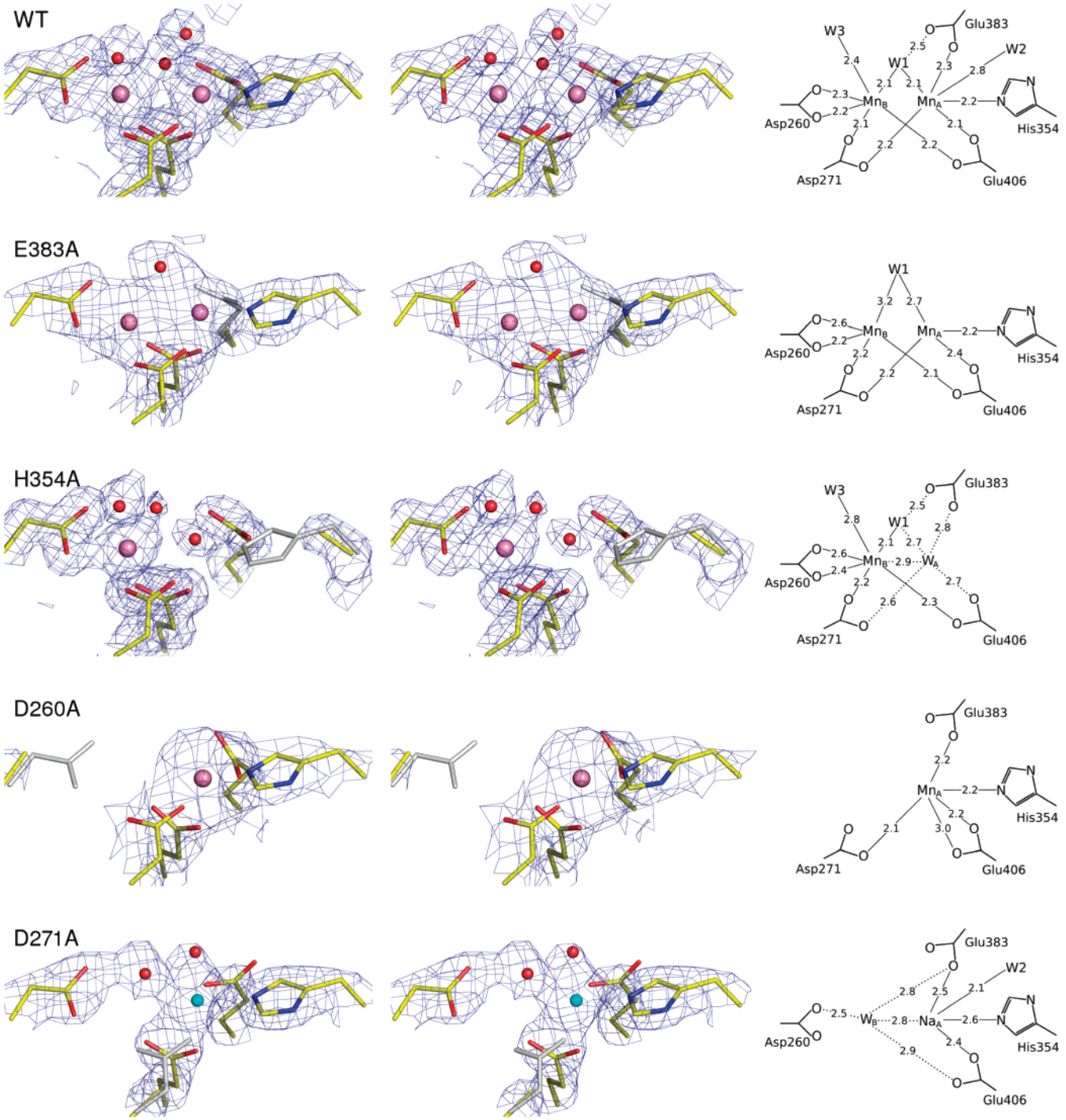

FIGURE 5: Stereoviews showing the active sites of *E. coli* APPro mutants in which metal−ligand residues are truncated to alanine (left) and schematic diagrams of the metal−ligand interactions (right). The wild-type enzyme [WT, PDB ID 1WL9 (*8*)] is shown for reference. For clarity, only the metal−ligand residues are shown. The conformation of the truncated side chain in the wild-type enzyme is shown in gray for the mutants. $2F_o - F_c$ electron density (1.5σ for WT, D260A, D271A, and E383A, 1.2σ for H354A) is shown in blue. Distances in the right column are in angstroms.

metal ions bound to the same set of ligands, and they are presumed to share a common mechanism of catalysis (*12*). All three enzymes cleave the N-terminal amino acid from a di- or oligopeptide. MetAP prefers substrates with methionine in the P_1 position, whereas the specificity of APPro and prolidase is shown by a preference for proline in the P_1' position. In this study, conserved residues at the active site of APPro likely to be involved in metal binding, substrate binding, or catalysis were mutated to alanine. The relationship between the activity of these mutants and the role of the mutated residues in wild-type APPro can now be discussed.

Substrate Binding at the Active Site of APPro. Consistent with its N-terminal specificity, APPro binds directly to the N-terminal amino group of a peptide substrate. In structures of APPro in complex with apstatin, of prolidase in complex with AHMH-Pro, and of MetAP in complex with AHHpA-peptide, the primary amino group of the peptide-like inhibitors is observed to bind to M_B, one of the two active site metal atoms (*10*, *20*, *22*). However, MetAP and APPro from

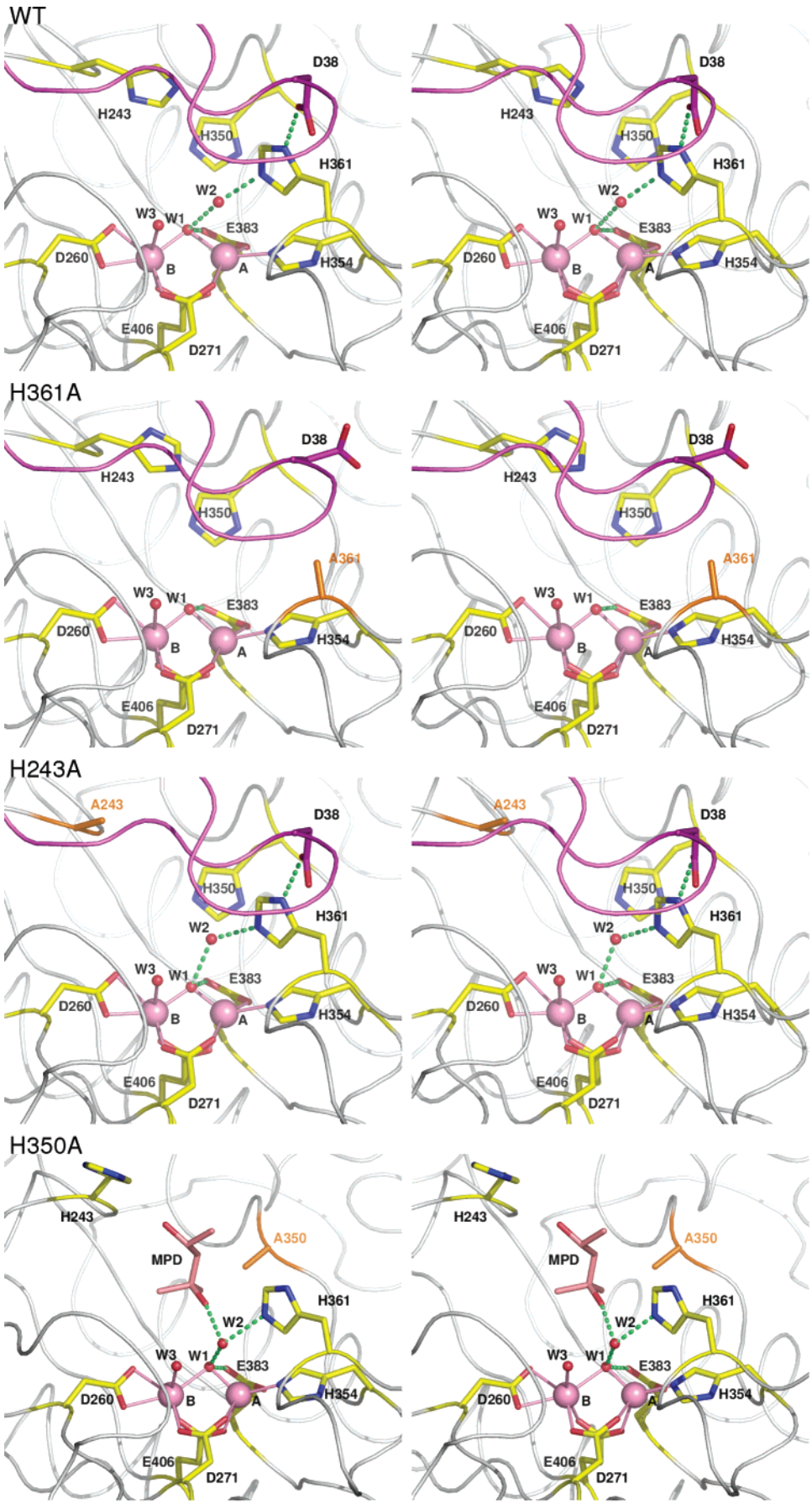

FIGURE 6: Active site of *E. coli* APPro mutants in which nonmetal−ligand residues are truncated to alanine. The wild-type enzyme [WT, PDB ID 1WL9 (*8*)] is shown for reference. For clarity, only solvent molecules that interact with the Mn(II) atoms of the dinuclear metal center (pink) are shown. The mutated residue is shown in orange, and the side chain of Asp38 from an adjacent subunit, which interacts with His361, is shown in purple (omitted in H350A for clarity).

selected species have been shown to be fully active with only the other metal, M_A, bound at the active site (*13*, *15*). It has been suggested that, in the absence of M_B, the positively charged amino group of the substrate binds to the carboxyl side chains that are usually ligands of M_B (*12*, *13*, *15*, *23*). This hypothesis is supported by the structure of apo-APPro in complex with the tripeptide Val-Pro-Leu, where the amino group of the substrate interacts with the side chains of Asp260 and Asp271 (*8*). Despite the fact that Mn_A (the metal atom invoked in mechanisms describing APPro single-metal activity) is present in D260A APPro, the mutant enzyme is inactive (Figure 2). This presumably arises from an inability to bind substrate, since neither Mn_B nor the carboxylate of Asp260 is available to interact with the amino group of the P_1 residue.

Interaction between the P_1' residue of the substrate and His243 is also required for catalysis. Mutation of His243 to alanine abolishes APPro activity (Figure 2), as does the equivalent H79A mutation in *E. coli* MetAP (*22*). In the apstatin complex of APPro, $N^{\epsilon 2}$(His243) acts as the donor in a hydrogen bond to the P_1' O(peptide) atom (*20*). An equivalent hydrogen bond is present in the complex of apo-APPro with the substrate Val-Pro-Leu (*8*) and in complexes of prolidase and MetAP with AHMH-Pro and AHHP-peptide, respectively (*10*, *22*). An obvious conclusion is that this hydrogen bond stabilizes substrate binding.

However, an alternate role for His243 has been proposed on the basis of the structure of *E. coli* MetAP in complex with the catalytic intermediate analogue L-methionine phosphonate. In this complex, MetAP $N^{\epsilon 2}$(His79) [equivalent to $N^{\epsilon 2}$(His243) of *E. coli* APPro] moves significantly from its position in the native enzyme and *donates* a hydrogen bond to a phosphonate oxygen of the ligand that is assumed to be in an equivalent position to the N(peptide) atom of the substrate P_1' residue (*21*). This analysis led to the proposal that MetAP $N^{\epsilon 2}$(His79) *accepts* a hydrogen bond from the P_1' peptide NH of the substrate (*21*) and that the same is true for the equivalent residue His243 in APPro (*12*). However, like APPro and prolidase, MetAP is active against substrates with proline in the P_1' position (*24*), and the peptide nitrogen of proline has no proton to donate in the formation of a hydrogen bond with His243 (or His79 in MetAP) (*8*, *20*). We therefore conclude that the essential catalytic role of His243, and equivalent residues in the related metalloenzymes, is stabilization of substrate binding by the *donation* of a hydrogen bond from $N^{\epsilon 2}$(His243) to the O(peptide) atom of the P_1' residue of the substrate.

APPro and prolidase have a strong preference for Xaa-Pro(-...) substrates. We have now shown that, like in dipeptidyl peptidase IV, which removes N-terminal Xaa-Pro dipeptides, and prolyl aminopeptidase, which cleaves the N-terminal Pro−Xaa bond, proline specificity in APPro arises from interactions of the enzyme with the distinctive prolidyl ring rather than from the special chemistry of Xaa−Pro peptide bonds (*27*, *28*). In structures of APPro in complex with the product dipeptide Pro-Leu, the substrate tripeptide Val-Pro-Leu, and the substrate-like inhibitor apstatin, a hydrophobic pocket cradles the prolidyl ring of the P_1' residue (*6*, *8*, *20*). The two residues that define the hydrophobic proline-binding pocket of *E. coli* APPro, His350 and Arg404, are conserved in 249 APPro and prolidase sequences (Table 1 and Supporting Information). Unlike the fully conserved, catalytically essential residues (the metal ligands, His243, and His361), His350 and Arg404 are not conserved in MetAP (*20*), lending further weight to the suggestion that their role is in determination of proline specificity. The side chains of His350 and Arg404 make van der Waals interactions with the C^{β} and C^{γ} atoms and the C^{γ} and C^{δ} atoms, respectively, of a bound proline residue (*8*). Analysis of this S_1' substrate binding pocket revealed that its size prohibits the binding of β-branched hydrophobic residues such as valine, explaining the lack of APPro activity toward such substrates (*8*). However, these structural analyses did not offer a facile explanation for the inability of APPro to efficiently cleave peptides with smaller residues (e.g., alanine) at the P_1' site.

New data presented in this paper directly address the issue of proline specificity in APPro. First, mutation of His350 to alanine reduces both the substrate-binding affinity and the catalytic activity of the enzyme (Figure 2). The structures of H350A and wild-type APPro differ only slightly. The observed difference in position of the side chain of His243 is unlikely to be significant as this residue is disordered or mobile in the absence of active site ligands (such as substrate or product) (*6*−*8*). Given that the imidazole side chain of His350 and the prolidyl ring of bound substrate or product form extensive hydrophobic contacts (*8*), we suggest that the reduced activity and poorer substrate binding of H350A *E. coli* APPro reflects its inability to hold the substrate in the correct orientation for catalysis. Mutations of the equivalent residue in porcine membrane-bound APPro (His519) to lysine or leucine also cause significant increases in K_M and, in the case of H519K, a significant decrease in k_{cat} (*19*).

Second, the reduced affinity of APPro for substrates with alanine or *N*-methylalanine at the P_1' position demonstrates that the proline residue is critical for substrate recognition. While Ala-Pro-Ala is able to competitively inhibit hydrolysis of the fluorogenic substrate Lys(Abz)-Pro-Pro-pNA with moderate efficiency ($IC_{50} = 0.22 \pm 0.05$ mM), no inhibition is seen in the presence of Ala-(*N*-methyl)Ala-Ala or Ala-Ala-Ala at concentrations up to 5 mM (Figure 3). Low levels of APPro activity against Xaa-Ala-... peptides (Figure 4 and refs *33* and *43*) show that the S_1' subsite of APPro can bind residues smaller than Pro, albeit weakly, and that such substrates are hydrolyzed. The activity of APPro depends linearly on concentrations of Ala-(*N*-methyl)Ala-Ala or Ala-Ala-Ala from 0 to 4 mM, confirming the low affinity of APPro for these peptides since they fail to saturate the enzyme. The importance of the C^{δ} atom of the P_1' proline residue for substrate recognition is highlighted by the observation that APPro cleaves Ala-(*N*-methyl)Ala-Ala more than an order of magnitude more readily than it does Ala-Ala-Ala.

Mechanism of Catalysis. Several similar mechanisms have been proposed for the pita bread metalloenzymes APPro and MetAP (*6*, *12*, *23*, *44*). Although these enzymes were originally identified as requiring two metal atoms for catalysis, at least some can function with only one metal at the active site (*13*−*15*, *45*). The principal features of the mechanistic proposals are common to both one- and two-metal forms of the enzymes. A solvent molecule, polarized by binding to one or both metal ions, is positioned for nucleophilic attack on the carbonyl carbon of the scissile peptide bond (*6*, *12*, *21*, *23*). A base, Glu383 in APPro,

Scheme 1: Proposed Catalytic Mechanism for *E. coli* APPro

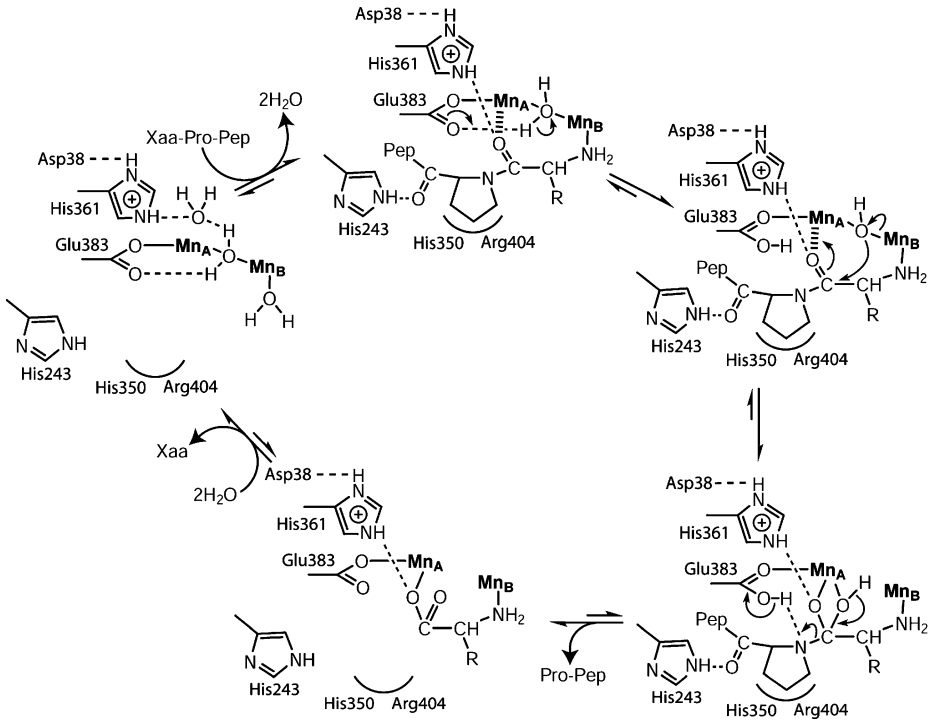

abstracts a proton from this nucleophile (*12*, *23*). The peptide carbonyl oxygen of the scissile peptide bond is coordinated directly to the "tightly" bound metal M_A (*12*, *23*). His361, originally identified as being required in the stabilization of an oxyanion intermediate (*6*, *21*), has recently been implicated in modulation of the Lewis acidity of the active site metal(s) (*23*). The current study presents a comprehensive survey of the effect of mutagenesis of conserved active site residues upon the structure and function of a pita bread metalloenzyme.

Mutation of any one of the metal-binding residues (Asp260, Asp271, His354, or Glu383) to alanine reduces APPro activity by at least 2 orders of magnitude (Figure 2), as previously observed for equivalently mutated forms of porcine membrane-bound APPro (*19*) or *E. coli* MetAP (*18*). Truncation of the side chains of these metal−ligand residues to alanine selectively abolishes binding of either or both Mn(II) atoms at the active site of APPro (Figure 5). In wild-type APPro, Asp271 bridges the two Mn(II) atoms. Neither Mn(II) atom is bound at the active site of D271A APPro, but an Na(I) atom from the crystallization buffer is located in the Mn_B site. Clearly, the D271A mutant is inactive because it lacks a metal atom capable of polarizing a solvent molecule as is required for catalysis (*8*).

Asp260 coordinates Mn_B in a symmetrical bidentate fashion in the wild-type enzyme. In the D260A mutant of APPro, Mn(II) is bound only at the M_A site. As explained earlier, D260A APPro is not able to function as an active single-metal form of the enzyme since, in the absence of Mn_B, the carboxyl group of Asp260 is required for binding of the terminal amino group of the substrate.

His354 coordinates Mn_A in the wild-type enzyme via its $N^{\epsilon 2}$ atom. Mutation of His354 to alanine results in the loss of Mn_A binding, and Mn_B binds with only 75% occupancy. Reduced occupancy of Mn_B is consistent with some cooperativity of metal binding. The loss of Mn_A prevents the proposed polarizing bond from the metal to the P_1 O(peptide) atom of the substrate (*23*), such that the P_1 carbonyl is no longer susceptible to nucleophilic attack.

Glu383 binds to Mn_A and forms a hydrogen bond with the bridging solvent atom in wild-type APPro. In E383A APPro both Mn(II) atoms are still present at the active site. The bridging solvent atom W1 is also present, but it is farther from the Mn(II) atoms than in the wild-type enzyme (Figure 5). Inactivity of E383A APPro may be caused by the removal of the base that deprotonates the bridging solvent nucleophile or by the movement of the nucleophile in the absence of the stabilizing bond from Glu383 to a position inappropriate for attack on the carbonyl carbon of the substrate.

Although not involved directly in metal binding, His361 is conserved in sequences of APPro, prolidase, and MetAP (*20*). Two roles have been proposed for His361 in the catalytic mechanism: modulation of the Lewis acidity of the active site metal atoms and/or stabilization of the *gem*-diol intermediate (*6*, *12*, *21*, *23*). The mutant enzyme H361A APPro has <1% of wild-type activity (Figure 2), and mutation of the equivalent residue in *E. coli* MetAP (His178) to alanine reduces the activity of the enzyme by about 2 orders of magnitude (*23*). Both Mn(II) atoms are present at the active site of H361A APPro, occupying the same positions as in the wild-type enzyme. This is consistent with isothermal titration calorimetry analysis of *E. coli* MetAP, which showed that the H178A mutation (equivalent to *E. coli* APPro H361A) does not disrupt metal binding (*23*). However, mutation of His361 to alanine has a subtle effect on the solvent structure at the active site of APPro. In the wild-type enzyme, the solvent molecule W2, near but not coordinated to Mn_A, forms hydrogen bonds to the bridging solvent molecule and His361 (Figure 6). In H361A APPro, W2 is not present at the active site (Figure 6). It has been suggested on the basis of Co(II) electronic absorption spectra that the nucleophilic hydroxide ion is more easily generated

in H178A MetAP than in the wild-type enzyme due to the loss of the strong hydrogen bond between the bridging solvent and W2, which has the effect of reducing the Lewis acidity of the Co(II) atoms and hence their ability to polarize the carbonyl bond of bound substrate (*23*). While this is consistent with the loss of W2 in H361A APPro, this suggestion may not be relevant for the catalytic mechanism. In complexes of wild-type APPro with the substrate analogue inhibitor apstatin and of *apo* APPro with the tripeptide substrate Val-Pro-Leu, W2 is displaced and a direct hydrogen bond is formed from $N^{\epsilon 2}$(His361) to the O(peptide) atom of the P_1 substrate residue (*8*, *20*). The orientation of the imidazole ring of His361 is stabilized by a hydrogen bond between $N^{\delta 1}$(His361) and the side chain carboxyl group of Asp38 of an adjacent subunit (Figure 6). In the structures of APPro in complex with substrate or product (*8*, *20*) the hydrogen bonds between the imidazole ring of His361, the P_1 O(peptide) atom, and the carboxylate group of Asp38 are maintained, and the imidazole ring of His361 is therefore in the doubly protonated form. Given that W2 is displaced when substrate binds, any modulation of the Lewis acidity of the metals in the resting enzyme is not likely to be important for catalysis. The hydrogen bond between the doubly protonated His361 and the P_1 O(peptide) atom observed in the structures of APPro in complex with apstatin and Val-Pro-Leu supports a role for this residue both in optimally positioning the scissile peptide bond for nucleophilic attack and in stabilizing the *gem*-diol intermediate.

Based upon these kinetic and structural data, an amended catalytic mechanism for APPro is presented in Scheme 1. Our proposal differs from published mechanisms for MetAP (*12*, *23*, *44*) only in the proposed roles of His243 and His361. The required P_1' proline residue of substrate is bound in a hydrophobic pocket, formed by His350 and Arg404, which correctly orients the substrate for catalysis. $N^{\epsilon 2}$(His243) forms a hydrogen bond with the P_1' O(peptide) atom, further stabilizing the substrate complex. The amino group of the P_1 substrate residue coordinates to Mn_B. In single-metal forms of the enzyme it is likely that the carboxylate side chains of Asp271 and Asp260 perform the function of Mn_B, binding substrate via salt bridges with the same amino group. The O(peptide) atom of the P_1 residue binds to Mn_A, polarizing the carbonyl bond to facilitate nucleophilic attack by the bridging solvent nucleophile. Glu383 abstracts a proton from the nucleophile. His361 and Mn_A stabilize the *gem*-diol intermediate that is formed following the nucleophilic attack. In the final step, collapse of this intermediate to products is facilitated by donation of the abstracted proton from Glu383 to the P_1' amine leaving group.

ACKNOWLEDGMENT

We thank Drs. Paul Curmi and Stephen Harrop for synchrotron data collection and Drs. Mibel Aguilar, Simon Easterbrook-Smith, and Rebecca Lee for helpful discussion on enzyme kinetics.

SUPPORTING INFORMATION AVAILABLE

Alignment of 249 APPro and prolidase sequences as a CLUSTAL formatted file and one table of mutagenic PCR primers. This material is available free of charge via the Internet at http://pubs.acs.org.

REFERENCES

1. Schechter, I., and Berger, A. (1967) On the size of the active site in proteases. I. Papain, *Biochem. Biophys. Res. Commun. 27*, 157−162.
2. Yaron, A. (1987) The role of proline in the proteolytic regulation of biologically active peptides, *Biopolymers 26*, S215−S222.
3. Ersahin, C., Euler, D. E., and Simmons, W. H. (1999) Cardioprotective effects of the aminopeptidase P inhibitor apstatin: studies on ischemia/reperfusion injury in the isolated rat heart, *J. Cardiovasc. Pharmacol. 34*, 604−611.
4. Kitamura, S., Carbini, L. A., Simmons, W. H., and Scicli, A. G. (1999) Effects of aminopeptidase P inhibition on kinin-mediated vasodepressor responses, *Am. J. Physiol. 276*, H1664−H1671.
5. Wolfrum, S., Richardt, G., Dominiak, P., Katus, H. A., and Dendorfer, A. (2001) Apstatin, a selective inhibitor of aminopeptidase P, reduces myocardial infarct size by a kinin-dependent pathway, *Br. J. Pharmacol. 134*, 370−374.
6. Wilce, M. C. J., Bond, C. S., Dixon, N. E., Freeman, H. C., Guss, J. M., Lilley, P. E., and Wilce, J. A. (1998) Structure and mechanism of a proline-specific aminopeptidase from *Escherichia coli*, *Proc. Natl. Acad. Sci. U.S.A. 95*, 3472−3477.
7. Graham, S. C., Lee, M., Freeman, H. C., and Guss, J. M. (2003) An orthorhombic form of *Escherichia coli* aminopeptidase P at 2.4 Å resolution, *Acta Crystallogr., Sect. D: Biol. Crystallogr. 59*, 897−902.
8. Graham, S. C., Bond, C. S., Freeman, H. C., and Guss, J. M. (2005) Structural and functional implications of metal ion selection in aminopeptidase P, a metalloprotease with a dinuclear metal center, *Biochemistry 44*, 13820−13836.
9. Bazan, J. F., Weaver, L. H., Roderick, S. L., Huber, R., and Matthews, B. W. (1994) Sequence and structure comparison suggest that methionine aminopeptidase, prolidase, aminopeptidase P, and creatinase share a common fold, *Proc. Natl. Acad. Sci. U.S.A. 91*, 2473−2477.
10. Maher, M. J., Ghosh, M., Grunden, A. M., Menon, A. L., Adams, M. W., Freeman, H. C., and Guss, J. M. (2004) Structure of the prolidase from *Pyrococcus furiosus*, *Biochemistry 43*, 2771−2783.
11. Roderick, S. L., and Matthews, B. W. (1993) Structure of the cobalt-dependent methionine aminopeptidase from *Escherichia coli*: A new type of proteolytic enzyme, *Biochemistry 32*, 3907−3912.
12. Lowther, W. T., and Matthews, B. W. (2002) Metalloaminopeptidases: common functional themes in disparate structural surroundings, *Chem. Rev. 102*, 4581−4607.
13. Cottrell, G. S., Hooper, N. M., and Turner, A. J. (2000) Cloning, expression, and characterization of human cytosolic aminopeptidase P: a single manganese(II)-dependent enzyme, *Biochemistry 39*, 15121−15128.
14. Hooper, N. M., Hryszko, J., Oppong, S. Y., and Turner, A. J. (1992) Inhibition by converting enzyme inhibitors of pig kidney aminopeptidase P, *Hypertension 19*, 281−285.
15. D'Souza, V. M., Bennett, B., Copik, A. J., and Holz, R. C. (2000) Divalent metal binding properties of the methionyl aminopeptidase from *Escherichia coli*, *Biochemistry 39*, 3817−3826.
16. Ghosh, M., Grunden, A. M., Dunn, D. M., Weiss, R., and Adams, M. W. (1998) Characterization of native and recombinant forms of an unusual cobalt-dependent proline dipeptidase (prolidase) from the hyperthermophilic archaeon *Pyrococcus furiosus*, *J. Bacteriol. 180*, 4781−4789.
17. Klinkenberg, M., Ling, C., and Chang, Y. H. (1997) A dominant negative mutation in *Saccharomyces cerevisiae* methionine aminopeptidase-1 affects catalysis and interferes with the function of methionine aminopeptidase-2, *Arch. Biochem. Biophys. 347*, 193−200.
18. Chiu, C. H., Lee, C. Z., Lin, K. S., Tam, M. F., and Lin, L. Y. (1999) Amino acid residues involved in the functional integrity of *Escherichia coli* methionine aminopeptidase, *J. Bacteriol. 181*, 4686−4689.
19. Cottrell, G. S., Hyde, R. J., Lim, J., Parsons, M. R., Hooper, N. M., and Turner, A. J. (2000) Identification of critical residues in the active site of porcine membrane-bound aminopeptidase P, *Biochemistry 39*, 15129−15135.
20. Graham, S. C., Maher, M. J., Simmons, W. H., Freeman, H. C., and Guss, J. M. (2004) Structure of *Escherichia coli* aminopeptidase P in complex with the inhibitor apstatin, *Acta Crystallogr., Sect. D: Biol. Crystallogr. 60*, 1770−1779.
21. Lowther, W. T., Zhang, Y., Sampson, P. B., Honek, J. F., and Matthews, B. W. (1999) Insights into the mechanism of *Escheri-*

chia coli methionine aminopeptidase from the structural analysis of reaction products and phosphorus-based transition-state analogues, *Biochemistry 38*, 14810−14819.
22. Lowther, W. T., Orville, A. M., Madden, D. T., Lim, S., Rich, D. H., and Matthews, B. W. (1999) *Escherichia coli* methionine aminopeptidase: implications of crystallographic analyses of the native, mutant, and inhibited enzymes for the mechanism of catalysis, *Biochemistry 38*, 7678−7688.
23. Copik, A. J., Swierczek, S. I., Lowther, W. T., D'Souza, V. M., Matthews, B. W., and Holz, R. C. (2003) Kinetic and spectroscopic characterization of the H178A methionyl aminopeptidase from *Escherichia coli*, *Biochemistry 42*, 6283−6292.
24. Hirel, P. H., Schmitter, M. J., Dessen, P., Fayat, G., and Blanquet, S. (1989) Extent of N-terminal methionine excision from *Escherichia coli* proteins is governed by the side-chain length of the penultimate amino acid, *Proc. Natl. Acad. Sci. U.S.A. 86*, 8247−8251.
25. Lin, L.-N., and Brandts, J. F. (1979) Evidence suggesting that some proteolytic enzymes may cleave only the trans form of the peptide bond, *Biochemistry 18*, 43−47.
26. Lin, L.-N., and Brandts, J. F. (1979) Role of cis−trans isomerism of the peptide bond in protease specificity. Kinetic studies on small proline-containing peptides and on polyproline, *Biochemistry 18*, 5037−5042.
27. Thoma, R., Loffler, B., Stihle, M., Huber, W., Ruf, A., and Hennig, M. (2003) Structural basis of proline-specific exopeptidase activity as observed in human dipeptidyl peptidase-IV, *Structure 11*, 947−959.
28. Inoue, T., Ito, K., Tozaka, T., Hatakeyama, S., Tanaka, N., Nakamura, K. T., and Yoshimoto, T. (2003) Novel inhibitor for prolyl aminopeptidase from *Serratia marcescens* and studies on the mechanism of substrate recognition of the enzyme using the inhibitor, *Arch. Biochem. Biophys. 416*, 147−154.
29. Altschul, S. F., Madden, T. L., Schaffer, A. A., Zhang, J., Zhang, Z., Miller, W., and Lipman, D. J. (1997) Gapped BLAST and PSI-BLAST: a new generation of protein database search programs, *Nucleic Acids Res. 25*, 3389−3402.
30. Bairoch, A., Apweiler, R., Wu, C. H., Barker, W. C., Boeckmann, B., Ferro, S., Gasteiger, E., Huang, H., Lopez, R., Magrane, M., Martin, M. J., Natale, D. A., O'Donovan, C., Redaschi, N., and Yeh, L. S. (2005) The Universal Protein Resource (UniProt), *Nucleic Acids Res. 33*, D154−D159.
31. Thompson, J. D., Gibson, T. J., Plewniak, F., Jeanmougin, F., and Higgins, D. G. (1997) The CLUSTAL-X windows interface: flexible strategies for multiple sequence alignment aided by quality analysis tools, *Nucleic Acids Res. 25*, 4876−4882.
32. Stöckel-Maschek, A., Stiebitz, B., Koelsch, R., and Neubert, K. (2003) A continuous fluorimetric assay for aminopeptidase P detailed analysis of product inhibition, *Anal. Biochem. 322*, 60−67.
33. Harbeck, H. T., and Mentlein, R. (1991) Aminopeptidase P from rat brain. Purification and action on bioactive peptides, *Eur. J. Biochem. 198*, 451−458.
34. Leslie, A. G. W. (1992) Mosflm−a programme for processing X-ray diffraction data, *Joint CCP4 + ESF-EAMCB Newsletter on Protein Crystallography, No. 26*.
35. Evans, P. R. (1997) Scala, *Joint CCP4 + ESF-EAMCB Newsletter on Protein Crystallography, No. 33*.
36. Murshudov, G. N., Vagin, A. A., and Dodson, E. J. (1997) Refinement of macromolecular structures by the maximum-likelihood method, *Acta Crystallogr., Sect. D: Biol. Crystallogr. 53*, 240−255.
37. Emsley, P., and Cowtan, K. (2004) Coot: Model-building tools for molecular graphics, *Acta Crystallogr., Sect. D: Biol. Crystallogr. 60*, 2126−2132.
38. Winn, M. D., Isupov, M. N., and Murshudov, G. N. (2001) Use of TLS parameters to model anisotropic displacements in macromolecular refinement, *Acta Crystallogr., Sect. D: Biol. Crystallogr. 57*, 122−133.
39. Vriend, G. (1990) WHAT IF: a molecular modeling and drug design program, *J. Mol. Graphics 8*, 52−56.
40. Lovell, S. C., Davis, I. W., Arendall, W. B., III, de Bakker, P. I., Word, J. M., Prisant, M. G., Richardson, J. S., and Richardson, D. C. (2003) Structure validation by Cα geometry: ϕ,ψ and Cβ deviation, *Proteins 50*, 437−450.
41. Schuttelkopf, A. W., and van Aalten, D. M. (2004) PRODRG: A tool for high-throughput crystallography of protein−ligand complexes, *Acta Crystallogr., Sect. D: Biol. Crystallogr. 60*, 1355−1363.
42. Kleywegt, G. J., and Jones, T. A. (1997) Detecting folding motifs and similarities in protein structures, *Methods Enzymol. 277*, 525−545.
43. Yoshimoto, T., Orawski, A. T., and Simmons, W. H. (1994) Substrate specificity of aminopeptidase P from *Escherichia coli*: Comparison with membrane-bound forms from rat and bovine lung, *Arch. Biochem. Biophys. 311*, 28−34.
44. Copik, A. J., Nocek, B. P., Swierczek, S. I., Ruebush, S., Jang, S. B., Meng, L., D'Souza, V. M., Peters, J. W., Bennett, B., and Holz, R. C. (2005) EPR and X-ray crystallographic characterization of the product-bound form of the Mn^{II}-loaded methionyl aminopeptidase from *Pyrococcus furiosus*, *Biochemistry 44*, 121−129.
45. Cosper, N. J., D'Souza, V. M., Scott, R. A., and Holz, R. C. (2001) Structural evidence that the methionyl aminopeptidase from *Escherichia coli* is a mononuclear metalloprotease, *Biochemistry 40*, 13302−13309.
46. Cruickshank, D. W. J. (1999) Remarks about protein structure precision, *Acta Crystallogr., Sect. D: Biol. Crystallogr. 55*, 583−601.
47. DeLano, W. L. (2002) *The PyMOL Molecular Graphics System*, DeLano Scientific, San Carlos, CA.

BI0518904